ORIGINAL PAPER

Structural and electrochemical impedance spectroscopic studies on reactive magnetron sputtered titanium oxynitride (TiON) thin films

P. Padmavathy · R. Ananthakumar ·
B. Subramanian · C. Ravidhas · M. Jayachandran

Abstract Titanium oxynitride films were deposited onto commercially pure titanium substrates by direct current reactive magnetron sputtering method using Ti targets and an Ar–N_2–O_2 mixture discharge gas. The X-ray photo-electron spectroscopy survey spectra on the etched surfaces of TiON films exhibited the characteristic Ti 2p, N 1s, and O 1s peaks at the corresponding binding energies 454.5, 397.0, and 530.7 eV, respectively. The surface topography of these coatings was studied using atomic force microscopy. The characteristic Raman peaks at 200 and 641 cm^{-1} for the TiN bonds and at 148, 398 ,and 518 cm^{-1} for the TiO_2 bonds were observed from the Laser Raman spectrometer. The potentiodynamic polarization studies in simulated bodily fluid were performed and the results are reported in this article.

Keywords Thin films · Magnetron Sputtering · XRD · AFM · XPS · Corrosion resistance

1 Introduction

Recently various surface coating technologies have been employed to enhance the important functional properties such as lubricity, biocompatibility, and antimicrobial effect for medical devices and surgical tools. Commercially pure titanium (CP-Ti) and Ti–6Al–4V remain as the two

P. Padmavathy · C. Ravidhas
Department of Physics, Bishop Heber College (Autonomous),
Tiruchirappalli 620 017, India

R. Ananthakumar · B. Subramanian (✉) · M. Jayachandran
CSIR-Central Electrochemical Research Institute,
Karaikudi 630 006, India
e-mail: subramanianb3@gmail.com

dominant titanium alloys used in implants. The stability of the oxide layer formed on CP Ti (and consequently its high corrosion resistance) and its relatively higher ductility (i.e., the ability to be cold worked), compared to Ti–6Al–4V, have led to the use of CP Ti in porous coatings (e.g., fiber metal) and total joint arthroplasty (TJA) components. Generally, joint replacement components (i.e., TJA systems) are made of Ti–6Al–4V rather than CP-Ti because of its superior mechanical properties. In recent years, metallic oxynitrides have become interesting research materials because of their remarkable optical and electronic properties, mechanical behavior, as well as chemical stability [1–3] and good adhesion to polymers, anti-reflective, decorative, and/or diffusion barrier coating for polymer components [4–6]. In recent studies [7, 8], they revealed properties common to both metallic TiN and semi-conducting TiO_2 compounds. Nowadays, the possibility to modify and control the surface wettability of biological materials has attracted significant scientific and technological interest. For biological systems, the nature of hydrophobic and hydration forces plays a key role on the mediation of solute adsorption and cell adhesion. Titanium oxide film is a widely used biocompatible material; therefore, modification of wetting behavior is of great importance for its biomedical application [9]. TiN coatings, on the contrary, are mostly used as protective and decorative coatings because of their extreme wear resistance and aesthetic golden color. In addition, TiN coatings serve as diffusion barriers due to their thermodynamic stability [10]. Indeed titanium oxynitrides exhibit the combined properties of metallic oxides (color, optical properties) and nitrides (hardness, wear resistance). Recently, interest in titanium oxynitride films has increased and have been extensively studied due to their improved physical and chemical properties, which mainly depend on their N/O

ratio. Oxygen-rich TiN_xO_y films have been used as insulating layer in metal–insulator–metal (MIM) capacitive structures to avoid interfacial oxide layer formation [11], while nitrogen-rich TiN_xO_y films have been used as an excellent diffusion barrier layer for semiconductor applications [12]; Additionally, many other useful applications of TiN_xO_y films, such as anti-reflective coating [13] and biomaterials [14] solar selective absorbers [15] and wear-resistant coatings [16], have been demonstrated. The wettability studies to determine hydrophilic or hydrophobic nature of titanium oxynitride film are the area that is unexplored and no literature has been found regarding the investigation of this property so far. TiN_xO_y films are the representative transition metal oxynitrides and can be deposited onto different substrates by various chemical vapor deposition (CVD) and physical vapor deposition (PVD) techniques with a tuneable N_yO ratio and consequently, with a wide range of physiochemical properties [17–19]. Reactive magnetron sputtering is specially an attractive process to deposit TiON films because of its several intrinsic advantages over CVD and PECVD process [20]. The main advantages include low-temperature deposition, large area deposition, and use of non-toxic gas. Sputtering of a titanium target in a mixed working gas (O_2 and N_2) or in a reactive gas atmosphere can be also used to obtain a tuneable N/O ratio in the films [3]. The purpose of this investigation is to deposit TiON films on CP-Ti substrates by direct current (DC) magnetron sputtering technique and to study the surface properties as well as their behavior in simulated bodily fluid.

2 Experimental

2.1 Substrate pretreatment

Titanium substrates were obtained using conventional turning and wire cut electric discharge machining (EDM) from commercially pure titanium rod conforming to ASTM B348 Grade 2. This was followed by a polishing process using silicone carbide emery papers (240–600 mesh sizes) to remove the turning marks and the recast zone generated by the EDM process. Final polishing was carried out using a centrifugal tumbling machine, by wet cut down, dry debarring, and ball burnishing. This process generated a surface finish better than 0.1-μm surface roughness (R_a), which is considered suitable for blood contact applications.

2.2 Deposition of TiON and their characterization

The layers of TiON were deposited on well-cleaned substrates using a DC magnetron sputter deposition unit HIND HIVAC. The base vacuum of the chamber was below

10^{-6} mbar and the substrate temperature was kept at 400 °C. High-purity argon was fed into the vacuum chamber for the plasma generation. The substrates were etched for 5 min at a dc power of 50 W and an argon pressure of 0.2 Pa. High-purity oxygen and nitrogen were used in equal proportion. The deposition parameters for TiON sputtering are summarized in Table 1.

The chemical nature of the outermost part of the films was investigated by X-ray photoelectron spectroscopy (XPS) using Multilab 2000. The XPS measurements were performed at a base pressure of 10^{-8} mbar using MgKα (X-ray of 1253.6 eV source). X-ray diffraction (XRD) was used to examine the changes in preferred grain orientation. XRD patterns were recorded with an X'pert pro diffractometer using Cu Kα (1.541 Å) radiation from 40-kV X-ray source running at 30 mA. The surface of the coatings was characterized by a molecular imaging Atomic Force Microscope (AFM). The Raman spectrum was recorded with a Renishaw InVia Laser Raman Spectrometer using an excitation wavelength of 632.8 nm. The data were collected with a 10-s data point acquisition time in the spectral region of 200–1000 cm^{-1}.

2.3 Electrochemical corrosion studies

Conventional three-electrode cell assembly was used for polarization studies as well as for impedance measurements. Electrochemical polarization studies were carried out using Autolab Electrochemical workstation. Experiments were conducted using the standard three-electrode configuration, with a platinum foil as the counter electrode, saturated calomel electrode as the reference electrode, and the coated and uncoated CP-Ti samples as the working electrode. The specimen (1.0 cm^2 exposed area) was immersed in the test solution of simulated bodily fluid (SBF) [21]. The composition of SBF is given in Table 2. Experiments were carried out at room temperature (28 °C). The system was allowed to attain a steady potential value for 10 min. The steady state polarization was carried out

Table 1 Optimized deposition parameters for TiON reactive sputtering

Objects	Specification
Target (2″ Dia)	Ti (99.9%)
Substrate	CP-Ti
Target to substrate distance	60 mm
Ultimate vacuum	1×10^{-6} m bar
Operating vacuum	2×10^{-3} m bar
Sputtering gas (Ar:N_2:O_2)	2:1:1 (TiON)
Power	200 W
Substrate temperature	400 °C

Table 2 Solution composition of simulated bodily fluid

Components	Concentration (g L^{-1})
NaCl	0.40
KCl	0.40
CaCl$_2$	0.795
MgCl$_2$	0.780
H$_2$NCONH$_2$	1.0
Egg white	0.005

from −550 mV versus SCE from the open circuit potential (OCP) and +200 mV versus SCE from the OCP separately using separate electrodes at a scan of 10 mV s^{-1}.

Electrodes of the same specification employed in polarization studies were used for impedance studies. In order to establish the OCP, prior to measurements, the sample was immersed in the solution for about 60 min. Impedance measurements were taken after attainment of steady state. An AC signal of 10 mV amplitude was applied and Impedance values were measured for frequencies from 0.01 Hz to 100 kHz.

3 Results and discussion

3.1 XPS analysis

The XPS survey spectra of 1 min etched surfaces of the TiON films (Fig. 1a) on CP-Ti substrate exhibited the characteristic Ti 2p, O 1s, and N 1s peaks at the corresponding binding energies 454.5, 530.6, and 397.0 eV, respectively [22]. The spectra confirm the presence of Ti–N and Ti–O$_2$ bondings in the deposited film. Initially at low power, less number of Ti atoms are sputtered from the Ti target, and only few Ti ions are created after sputtering due to charge exchange. These Ti ions will first react with O$_2$ due to their strong affinity. Therefore, the deposited film is mainly comprised Ti–O bonding. With increasing power more numbers of Ti atoms are sputtered from Ti target and large number of Ti ions are created due to charge exchange, which is more sufficient to form TiO$_2$ bonding leaving simply Ti ions, under this condition, there is more opportunity to form the Ti–N bonding also in addition to the preferentially formed Ti–O$_2$ bonding.

From high-resolution XPS measurements of the normal surface of the films, the spin orbit doublet Ti 2p1/2 and Ti 2p3/2 peaks at binding energies 460.5 and 454.5 eV, respectively, was found in the Ti spectra as shown in Fig. 1b. A linear type background subtraction was used. The spin–orbit doublet with binding energy of 454.9 eV (2p3/2) and 460.9 eV (2p1/2) are associated with TiN phase. The binding energies of the 2p3/2 (457.9 eV) and

2p1/2 (463.9 eV) levels of this doublet are corresponding to Ti–O bonds. The peak at 456.4 eV (2p3/2) is due to the formation of Ti–O–N bonding, which confirms the presence of TiO$_x$N$_y$ phase [23].

The C 1s peaks in the spectra (at 284.9 eV) may be the contribution from organic carbon which is unavoidable while using oil diffusion pump for evacuating the deposition chamber and XPS sample holding compartment [24]. Further, carbon contamination might have occurred due to the air contamination when the films were transferred from the sputtering instrument to the XPS sample chamber.

The presence of oxyhydroxides is strongly supported by the O 1s spectra, which is shown in Fig. 1c. A strong peak at 530.7 eV (contribution of O$_2$) indicates the characteristic of OH group. It can be supposed that due to the high reactivity of oxygen with Ti, its presence is caused by some minor oxidation during the deposition and, for a major part, to surface oxidation in air after the deposition. Obviously, the observed elevated coating roughness confirms the interaction of the surface with oxygen. N 1s spectrum showed peaks centered at 397.0 eV as shown in Fig. 1d. The low nitridation in the films may be due to high surface oxidation. The source of oxidation may be the nitrogen gas, the commercial nitrogen gas used here might have contained considerable percentage of oxygen impurities [25]. The Ar 2p peak identified in the spectra of the etched surface may be from the adsorbed argon during substrate etching or Ar species incorporated into the films during growth [26].

3.2 Structural analysis

Figure 2 shows the X-ray diffraction pattern of titanium oxynitride films deposited at 400 °C. The peak positions were compared with the JCPDS file No-03-065-5574 for TiN layers and No-00-089-4921 for TiO$_2$ layers and the corresponding planes were indexed. The TiN and TiO$_2$ layers have FCC and tetragonal structures, as indicated by the presence of (200), (220), and (101) peaks, respectively.

The typical 2D AFM images of TiON films are shown in Fig. 3. From the horizontal cross section analysis of AFM image with protruding tip structure, and laterally spreaded grain morphology, the minimum and maximum grain size was estimated to be in the range of 100–150 nm. Individual grains are clearly observed and closely packed indicating the vertically aligned axial arrangements of the crystals. The value of the mean roughness R_a was calculated as the deviations in height from the profile mean value [27].

3.3 Laser Raman studies

Raman scattering is a powerful and non-destructive technique to study the as-synthesized new materials. It can provide important evidence on the microstructure of films [28].
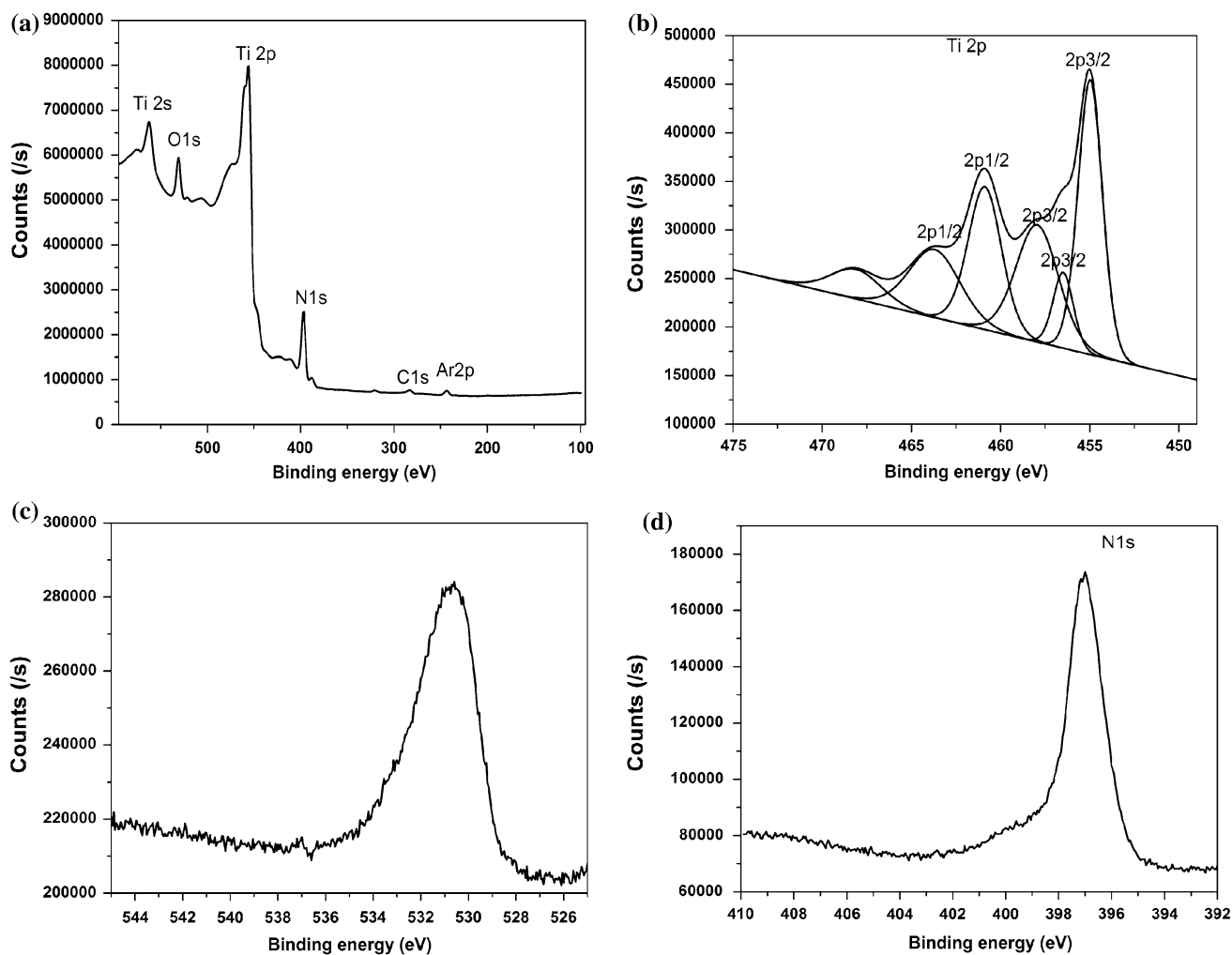
Fig. 1 XPS spectra of TiON film **a** survey scan, **b** narrow scan of Ti 2p, **c** O 1s and **d** N 1s
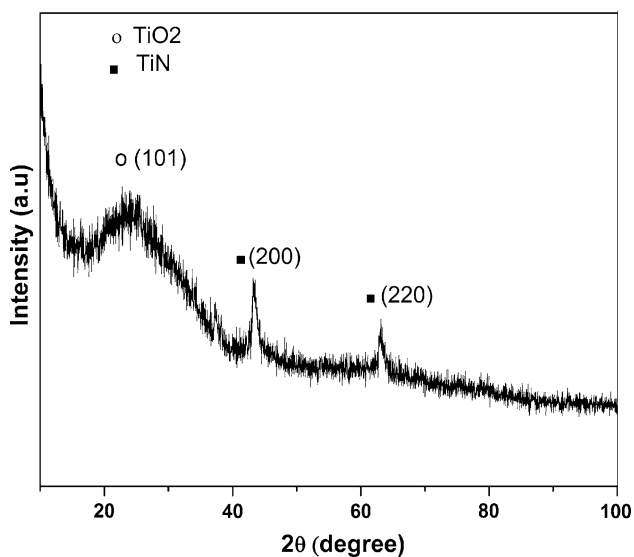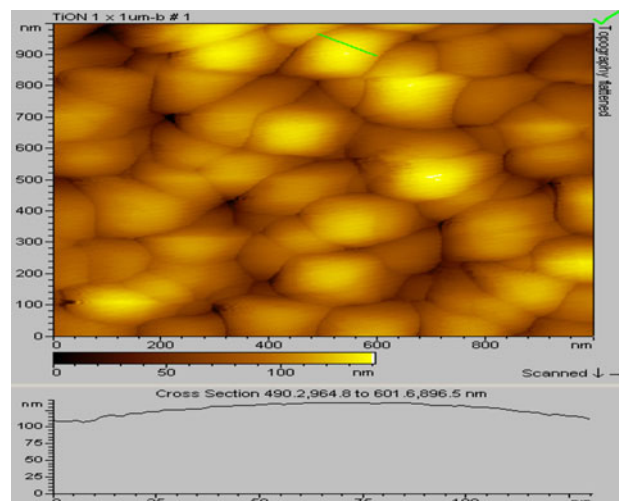

Fig. 2 X-ray diffraction pattern for TiON film
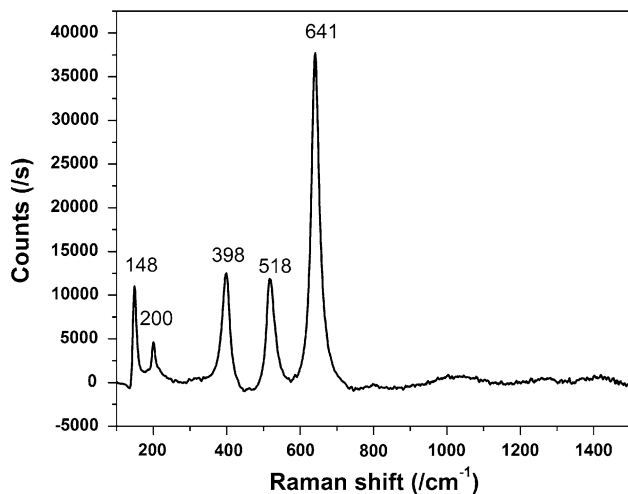

Fig. 3 AFM image of TiON thin film on CP-Ti

Fig. 4 Laser Raman spectra of TiON thin films on CP-Ti

Fig. 5 The potentiodynamic polarization curve in simulated bodily fluid solution for (*a*) CP-Ti substrate, (*b*) TiN and (*c*) TiON on CP-Ti

The Raman spectra in the range of 100–1100 cm^{-1} for TiON are shown in the Fig. 4. The peaks at 200 and 641 cm^{-1} arise from the first-order transverse acoustic (TA) and transverse optical (TO) modes of TiN bond, respectively. Peaks at 148 and 518 cm^{-1} are typical characteristics of rutile TiO$_2$ bonds [29]. Features at 398 cm^{-1} indicate the presence of anatase structure that coexists in the film [29].

3.4 Electrochemical corrosion behavior

The results of corrosion testing for the CP-Ti substrate, TiN and TiON in simulated bodily fluid solution are given in Table 3. The corrosion potential of the CP-Ti substrate is about −0.205 V. The positive shift of E_{corr} to −0.174 V for TiON indicates better corrosion resistance of the TiON coatings as shown in Fig. 5. The corrosion current I_{corr} of CP-Ti is greater than those of TiN and TiON. For the TiON, the corrosion current is reduced to 0.67 × 10^{-7} A cm^{-2}, as indicated in Table 3. The same three-electrode cell assembly, as used for the potentiodynamic polarization experiments, was employed for the AC impedance investigations. When the sample is immersed in the electrolyte the defects in the coating provide the direct diffusion path for the corrosive media. In this process, the galvanic corrosion cells are formed and the localized corrosion dominates the corrosion process. The electrochemical interface can be divided into two sub-interfaces: electrolyte/coating and electrolyte/substrate. The single semicircle behavior obtained for the samples is believed to
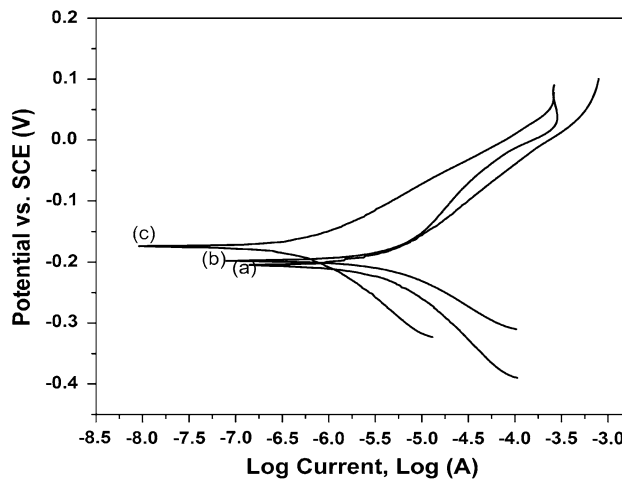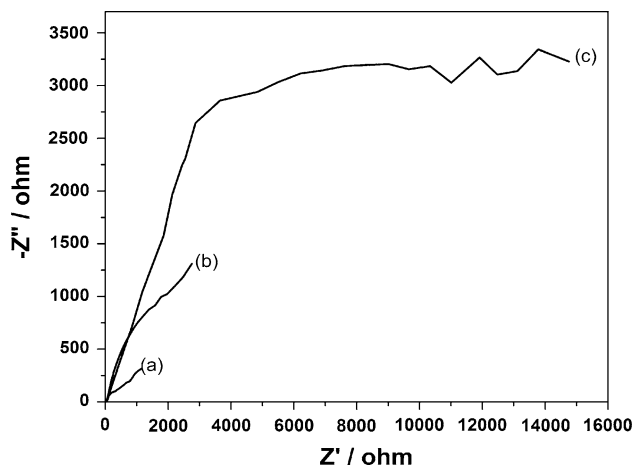

Fig. 6 Nyquist plots (*a*) CP-Ti substrate (*b*) TiN and (*c*) TiON on CP-Ti

be due to the short exposure time (60 min), which is not sufficient to reveal the degradation of the substrate [30]. The R_{ct} increases (Table 3) in the following order: TiON > TiN > CP-Ti, which shows (Fig. 6) that TiON coating on Ti substrate has higher corrosion resistance.

4 Conclusions

TiON thin films were successfully prepared using reactive direct current (DC) magnetron sputtering onto CP-Ti

Table 3 Polarization and electrochemical impedance data obtained for CP-Ti, TiN and TiON films substrate

Sample	E_{corr} (V)	I_{corr} (×10^{-7} A cm^{-2})	Corrosion rate (×10^{-3} mm y^{-1})	R_{ct} (Ω cm^2)	C_{dl} (×10^{-9} F cm^{-2})
CP-Ti	−0.205	8.13	28.3	1114.0	453.7
TiN	−0.198	1.34	5.2	2722.0	44.6
TiON	−0.174	0.67	3.1	14727.7	3.2

substrates. XPS analyses show that the prepared TiON films exhibited a mixture of Ti–N and Ti–O–N chemical binding states. For sample TiON, a two-phase structure with both FCC TiN (200) grains and tetragonal TiO_2 (101) grains are clearly evidenced, from XRD. Characteristic peaks of rutile and anatase structure of TiO_2 were found to coexist in the TiON film as observed from Laser Raman. The potentiodynamic polarization and EIS measurements showed that the TiON coatings on CP-Ti exhibited superior corrosion resistance when compared to the TiN and the bare CP-Ti substrate.

References

1. Chappe JM, Martin N, Lintymer J et al (2007) Appl Surf Sci 253:5312
2. Yang X, Li C, Yang B et al (2004) Chem Phys Lett 383:502
3. Vaz F, Cerqueira P, Rebouta L et al (2004) Thin Solid Films 447–448:449
4. Vaz F, Cerqueira P, Rebouta L et al (2003) Surf Coat Technol 174–175:197
5. Martin N, Banakh O, Santo AME et al (2001) Appl Surf Sci 185:123
6. Kazemeini MH, Berezin AA, Fukuhara N (2000) Thin Solid Film 372:70
7. Chappe JM, Martin N, Terwagne G et al (2003) Thin Solid Films 440:66
8. Jung MJ, Nam KH, Chung YM et al (2003) Surf Coat Technol 171:71
9. Lin Z, Liu K, Zhang YC et al (2009) Mater Sci Eng B 156:79
10. Mohamed SH, Kappertz O, Niemeier T et al (2004) Thin Solid Films 468:48
11. Pradhan SK, Reucroft PJ (2003) J Cryst Growth 250:588
12. Kim KH, Lee SH (1996) Thin Solid Films 283:165
13. Oyama T, Ohsaki H, Tachibana Y et al (1999) Thin Solid Films 351:235
14. Koerner RJ, Butterworth LA, Mayer IV (2002) Biomaterials 23:2835
15. Lazarov M, Raths P, Metzger H et al (1995) J Appl Phys 77:2133
16. Guillot J, Jouaiti A, Imhoff L et al (2002) Surf Interface Anal 33:577
17. Scopel WL, Fantini MCA, Alayo MI et al (2002) Thin Solid Films 413:59
18. Suzuki M, Saito Y (2001) Appl Surf Sci 173:171
19. Kazemeini MH, Berezin AA, Fukuhara N (2000) Thin Solid Films 372:70
20. Jiang N, Shen YG, Maia YW et al (2004) Mater Sci Eng B 106(2):163
21. Huang HH, Hsu CH, Pan SJ et al (2005) Appl Surf Sci 244:252
22. Vesel A, Mozetic M, Kovac J et al (2006) Appl Surf Sci 253:2941
23. Marco JF, Gancedo JR, Auger MA et al (2005) Surf Interface Anal 37:1082
24. Musher JN, Gordon RG (1996) J Electrochem Soc 143C:736
25. Wu HZ, Chou TC, Mishra A et al (1990) Thin Solid Films 191:55
26. Vargheese KD, Rao GM, Balasubramanian TV et al (2001) Mater Sci Eng B 83:242
27. Jacobs MH (1986) Surf Coat Technol 29:221
28. Shum PW, Zhou ZF, Li KY (2003) Surf Coat Technol 166:213
29. Shum PW, Li KY, Zhou ZF et al (2004) Surf Coat Technol 185(2–3):245
30. Liu C, Bi Q, Matthews A (2001) Corros Sci 43:1953